Talanta 155 (2016) 62–69

Contents lists available at ScienceDirect

Talanta

journal homepage: www.elsevier.com/locate/talanta

High fluorescence S, N co-doped carbon dots as an ultra-sensitive fluorescent probe for the determination of uric acid

Haiyan Wang, Qiujun Lu, Yuxin Hou, Yalan Liu, Youyu Zhang*

Key Laboratory of Chemical Biology and Traditional Chinese Medicine Research (Ministry of Education), College of Chemistry and Chemical Engineering, Hunan Normal University, Changsha 410081, PR China

ARTICLE INFO

Article history:
Received 24 January 2016
Received in revised form
8 April 2016
Accepted 9 April 2016
Available online 10 April 2016

Keywords:
S, N co-doped C-dots
Hydroxyl radicals
Uric acid
Serum samples

ABSTRACT

Sulfur, nitrogen co-doped carbon dots (S, N co-doped C-dots) as highly selective fluorescent probe for uric acid (UA) detection were designed. The S, N co-doped C-dots with high quantum yield of 73.1% were prepared by hydrothermal method. It was found that the fluorescence of S, N co-doped C-dots was quenched apparently by hydroxyl radicals from Fenton reaction between H_2O_2 and Fe^{2+}. The production of H_2O_2 originated from the oxidization of UA by uricase. Therefore, an optical biosensor was developed for the detection of UA based on Fenton reaction and enzymatic reaction. Under the optimized conditions, two linear relationships between the ratio of fluorescence quenching of the C-dots and UA concentration were found in the range of 0.08–10 μM and 10–50 μM, respectively. The detection limit was down to 0.07 μM. Moreover, the proposed biosensor was successfully applied to the detection of uric acid in human serum samples.

1. Introduction

Uric acid (UA) is a extremely important biological molecule as well as a main end product of purine metabolism in the human body [1]. For a healthy person, the concentration of UA should be in the range of 0.15–0.42 mM in the blood sample [2]. UA levels over this range may cause many diseases, such as gout, high blood pressure, kidney disease, leukemia, pneumonia, cardiovascular diseases, high cholesterol and multiple sclerosis [3,4]. Hence it is significantly important to detect the concentration of UA in biological fluids for the early stage warning of these conditions and for the diagnosis of patients. Recently, some methods including high performance liquid chromatography [5], mass fragementography [6], electrochemical techniques [7], chemiluminescence [8] and fluorescence (FL) method [9] have been developed for detecting of uric acid. Among these methods, FL sensing is a fast, simple and non-destructive operation method. Although some FL sensors have been reported to detect uric acid based on metal nanoclusters and semiconductor quantum dots [10, 11], these nanomaterials suffer from certain limitations such as high expense, poor aqueous solubility and weak FL intensity. Therefore, it is significantly important to develop new materials with excellent properties and suitable designs to gain sensors owning superior performance.

Fluorescence carbon dots (C-dots) are new promising carbon material, which have received increasingly concern from researchers due to their low toxicity, excellent chemical inertness, biocompatibility and high resistance to photobleaching. Recently, C-dots have been applied in chemical sensing [12], biosensing [13], bioimaging [14], nanomedicine [15], photocatalysis [16] and electrocatalysis [17] *etc*. However, the C-dots in the fields of FL sensors suffer from low fluorescence quantum yields (FLQY). To improve the FL property of C-dots, surface passivation and element doping have been widely explored. Surface passivation is usually carried out by attaching polymeric materials, such as oligomeric PEG, PEG_{1500N}, on an acid-treated C-dots surface to form a polymeric layer [18,19]. However, such modifications are complex to purify and not environmentally friendly. Compared to surface passivation, element doping is an effective method to improve FL property of C-dots because this method can improve unique electronic and optical characteristics of C-dots and provide more active sites on C-dots surface [20,21]. Furthermore, there are no need additional modified processes for the doping of C-dots. For instance, nitrogen doped carbon dots (N-doped C-dots) with FLQY of 13.5% were synthesized by Yang et al. [22]. Zhou et al. [23] reported that phosphorus doped carbon dots (P-doped C-dots) with FLQY of 25% were synthesized by a solvent-thermal method. Shan et al. [24] developed a facile one-pot solvothermal route for synthesis of FL B-doped carbon quantum dots (BCQDs) with FLQY of 14.8% using BBr_3 as the boron source and hydroquinone as the precursor. Although the FLQY of element-doped C-dots is higher than that of undoped C-dots, it is not enough to meet the requirements of high

* Corresponding author.
E-mail address: zhangyy@hunnu.edu.cn (Y. Zhang).

http://dx.doi.org/10.1016/j.talanta.2016.04.020
0039-9140/

sensitive for trace analysis. Therefore, it is significant to develop C-dots with excellent characters and high quantum yield. Compared with element-doped C-dots, dual-elements co-doped C-dots are scarcely reported. Li et al. [25] developed a double doping strategy of Mg/N double doped C-dots with citric acid, magnesium hydroxide and ethylenediamine as precursors. Paraknowitsch et al. [26] reported high temperature carbonized strategy of 1-Butyl-3-methyl-pyridinium-dicyanamide (BMP-dca) and tetra-alkyl-phosphonium-bromide to yield P, N co-doped C-dots. However, these methods suffer some defects of complex operating processes, high temperature and hard pure conditions for C-dots. Thus, it is significant to develop a facile and simply method for the preparation of co-doping C-dots with outstanding FL properties.

In this paper, we proposed a simple and efficient route to prepare S, N co-doped C-dots with a high FLQY of 73.1% through a one-pot hydrothermal method. The stability experiments show that S, N co-doped C-dots solution owns well properties of acid resistance, alkaline resistance, salt stability, photo-stability and resistance to photo-bleaching. The FL of S, N co-doped C-dots was quenched apparently by hydroxyl radicals from Fenton reaction. Based on the property of S, N co-doped C-dots, the Fenton reaction and enzymatic reaction of uric acid (UA), an eco-friendly, simple and selective fluorescent biosensor for UA was constructed (Scheme 1). The biosensor shows a wide linear detection range, good selectivity, and low detection limit and can be successfully applied to detect UA in human serum with satisfactory results.

2. Experimental section

2.1. Materials

Sodium citrate (CA), thiourea, hydrogen peroxide, sulfate iron, quinoline sulfate, KCl, NaCl and ammonium ferrous sulfate were obtained from Shanghai Reagent (Shanghai, China). Uric acid oxidase (UAO), uric acid (UA), ascorbic acid (AA), dopamine (DA), homocysteine (Hcys), cysteine (Cys), glutathione (GSH), lysine (Lys), lactose, glucose and leucine (Leu) were purchased from Sigma-Aldrich. The human serum was obtained from Hospital of Hunan Normal University. The standard UA solution is prepared using uric acid by dissolving in a small amount of 1 mol L^{-1} NaOH, fixed using PBS (0.01 M, pH 7.0), and stocked at 4 °C. FLQY is determined using a previously published procedure by using quinine sulfate as a reference standard (FLQY=54%). All other chemicals used in this work were of analytical grade. Millipore Milli-Q ultrapur water (Millipore, ≥ 18 MΩ cm^{-1}, U.S.A) is used throughout the experiments.

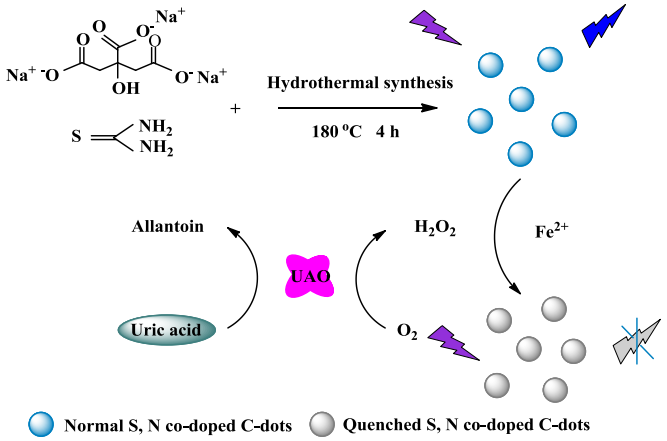

Scheme 1. Schematic of synthesis of S, N co-doped C-dots and proposed uric acid-sensing mechanism.

2.2. Apparatus

Transmission electron microscope (TEM) images were collected from a JEOL-1230 transmission electronic microscope (JEOL, Japan). The ultraviolet – visible (UV – vis) spectra were obtained by a UV-2450 UV – vis spectrophotometer (Shimazu Co., Japan). An F-7000 fluorescence spectrophotometer (Hitachi Co., Japan) was applied for the fluorescence analysis. Fourier transform infrared spectra (FT-IR) were recorded on a Nicolet Nexus 670 FT-IR spectroscope (Nicolet Instrument Co., USA). X-ray photoelectron spectroscopy (XPS) data for S, N co-doped C-dots was measured by a K-Alpha 1063 XPS (Thermo Fisher Co. U.K.) for analysis structure information of S, N co-doped C-dots. The ζ potential measurement of S, N co-doped C-dots before and after reaction with both H_2O_2 and Fe^{2+} were performed on the Nano-ZS Zetasizer ZEN3600 (Malvern Instruments Ltd., UK). Hitachi 7100 Automatic Biochemical Analyzer (Hitachi Co., Japan) was applied for the standard analysis of UA.

2.3. Preparation of S, N co-doped C-dots

The S, N co-doped C-dots were prepared by hydrothermal method using citric acid as carbon source and thiourea as both sulfur and nitrogen source. Briefly, 0.3 g citric acid and 0.6 g thiourea were firstly dissolved into 5 mL water to form a clear solution under the constantly stirring. Then the solution was transferred into a 25 mL Teflon lined stainless steel autoclave. Afterward, the sealed autoclave was heated to 180 °C in an electric oven and kept for 4 h. After naturally cooled to room temperature, the product was centrifuged at 10,000 rpm for 10 min to remove the large size particles and dialyzed against water through a dialysis bag (cut-off molecular weight 500 Da) for 2 days. The suspension of C-dots was finally obtained and stored at 4 °C for further characterization and applications.

2.4. Fluorescence quenching experiments with uric acid

A certain amount of S, N co-doped C-dots was diluted into 1 mL PBS solution (0.1 M, pH=4.0) (the final concentration of C-dots was 0.02 mg mL^{-1}). The fluorescence intensity was recorded (F_0). 100 μL UA solutions with different concentrations were prepared by diluting of different volume of standard UA solution using PBS solution (0.01 M, pH 7.0). Then, 10 μL UAO (1.3 U mL^{-1}) was added into the uric acid solution, and the mixture solution was incubated at 37 °C for 45 min. And then, 20 μL C-dots (the final concentration of C-dots was 0.02 mg mL^{-1}) was added to the above reaction solution. After pH value was adjusted to 4.0 with 1 M HCl, 30 μL of 0.01 M Fe^{2+} was added sequentially. Finally, the mixture was diluted to 1 mL with PBS (0.1 M, pH=4.0). The fluorescence intensity was recorded (F).

2.5. Analysis of practical samples

The human serums were obtained from Hospital of Hunan Normal University. These samples were adjusted to pH 7.0 with PBS to obtain desired serum concentration (the final concentration of serum was diluted 10-folds). All the samples were first incubated with uricase (1.3 U mL^{-1}) in PBS (0.1 M, pH=7.0) for 45 min at 37 °C bath. C-dots was 0.02 mg mL^{-1} dispersed in PBS, the pH of the solution was adjusted to 4.0 with 1 M HCl after addition of incubated serum and Fe^{2+} (0.3 mM). The incubation time of Fenton reaction is 15 min. The proposed method was applied to detect UA levels in human serum samples. According to the standard method (that is uricase-pod method). The

concentration of UA in each sample was also analyzed using an instrument (Hitachi 7100 Automatic Biochemical Analyzer) of Hospital of Hunan Normal University.

3. Results and discussion

3.1. Properties investigation of S, N co-doped C-dots

S, N co-doped C-dots were prepared by hydrothermal method using citric acid as carbon source and thiourea as both sulfur and nitrogen source. In order to obtain S, N co-doped C-dots owning excellent fluorescence properties, hydrothermal temperature, hydrothermal time and the mass ratio of sodium citrate (CA) and thiourea were optimized. The FLQY of as-prepared C-dots was investigated at different synthesis conditions and the results are listed in the supporting information (Table S1). The quinine sulfate solution (quantum yield 54%) was used as reference. Thus, the excellent C-dots with the highest FLQY could be obtained from hydrothermal reaction of 1:2 CA/thiourea at 180 °C for 4 h and be chosen as fluorescent probe for further application.

In order to investigate morphology and structure information of C-dots, a series of characterizations including transmission electron microscopy (TEM), high-resolution transmission electron microscopy (HRTEM), Fourier transform infrared spectra (FT-IR) and X-ray photoelectron spectroscopy (XPS) were recorded. As shown in Fig. 1A, TEM images show that S, N co-doped C-dots are of low size dispersity [27,28]. As shown in Fig. 1B, the size distributions of S, N co-doped C-dots indicate that the diameters rang from 4.0 to 6.0 nm. The HRTEM image of the C-dots shows a crystalline structure with a lattice spacing of 0.20 nm (inset in Fig. 1A), which attributes to the (100) diffraction planes of graphitic carbon [29]. FT-IR spectra of the prepared S, N co-doped C-dots are shown in Fig. C. The peak at 3339 cm^{-1} is identified as the stretching vibration absorption peak of the $–NH_2$ and –OH band [30]. The peak at 1721 cm^{-1} is related to the stretching vibration peak of C=O bond. The bending vibration of the C=C appears at 1593 cm^{-1}. The peak at 1230 cm^{-1} is related to the stretching vibration of C–N. The peak at 1230 cm^{-1} is ascribed to the stretching vibration of C–C, and C–S bond. The peak at 1045 cm^{-1} is attributed to the stretching vibration of C–O–C, C–O, C=S and S=O band [31–33]. The above observations confirm that reductive groups, such as –OH, $–NH_2$ and C–S, exist on S, N co-doped C-dots surface and indicate that sulfur and nitrogen are successfully doped into the C-dots. As shown in Fig. 1D, the XPS full scan spectra show that four clear peaks around 164 eV, 285 eV, 398.5 eV and 531 eV ascribe to sulfur, carbon, nitrogen, and oxygen, respectively [33]. As shown in Fig. S1A, the S_{2p} spectra mainly are made of two peaks centered at 164.0 eV and 167.6 eV, suggesting that sulfur exists in two forms. The former peak can be disintegrated into two distinct components at 163.5 eV and 164.6 eV, which agree with the reported $2p_{3/2}$ and $2p_{1/2}$ positions of the -C-S-covalent bond of the thiophene-S [34]. The later peaks at 167.6, 168.5, and 169.3 eV are related to -C-SO_x-(x=2,3,4) species [35]. The C_{1s} peaks at 284.5, 285.3, 286, 186.5 and 288.2 eV can be assigned to the form of C–C/C=C, C=S, C-N, C-O and C=O,

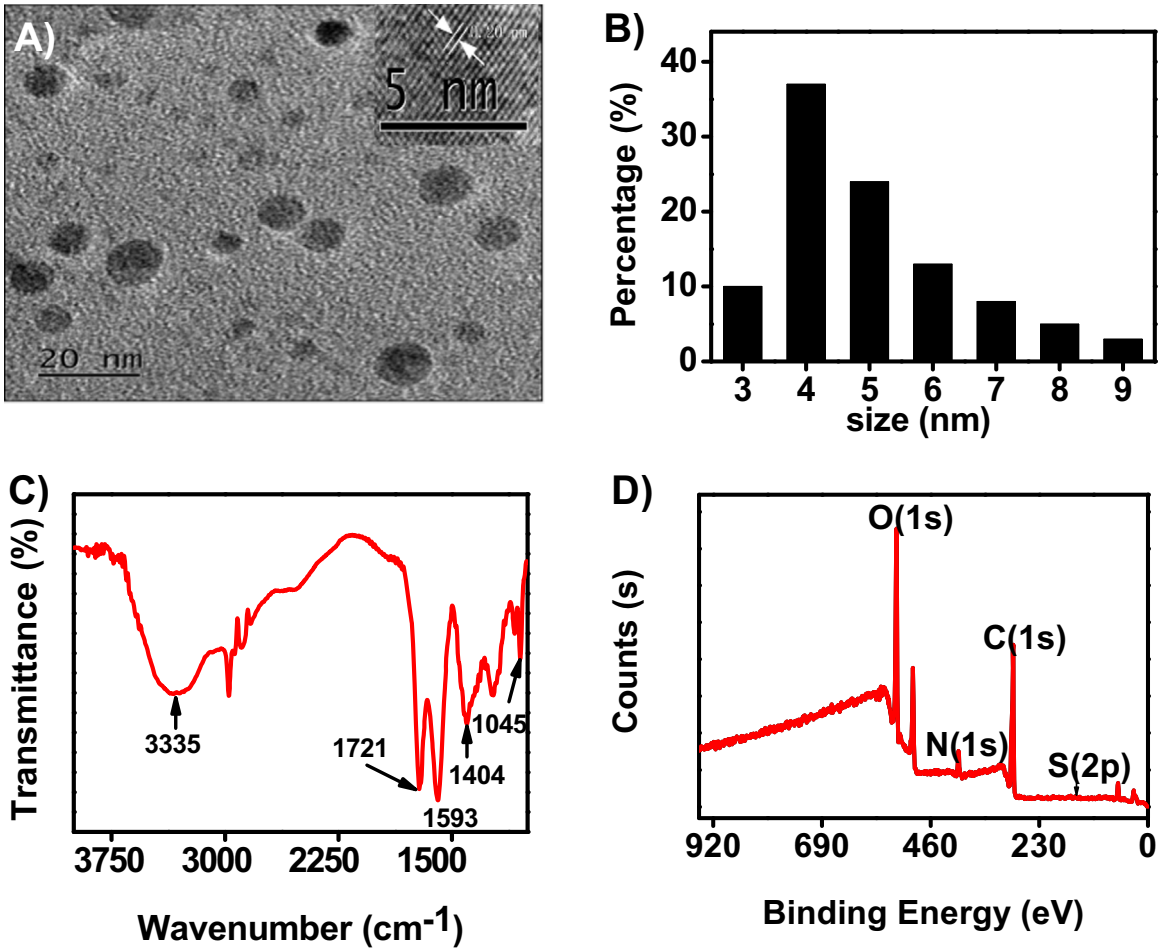

Fig. 1. (A) Typical TEM and HRTEM (inset) images of S, N co-doped C-dots. (B) Size distribution histograms of S, N co-doped C-dots. (C) FT-IR spectra of S, N co-doped C-dots. (D) XPS full spectra of S, N co-doped C-dots.

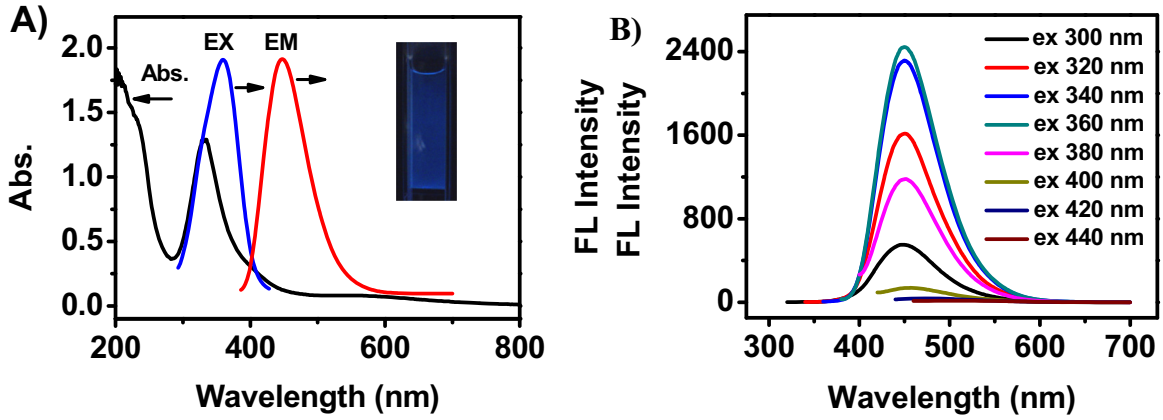

Fig. 2. (A) UV–vis spectra and FL spectra of S, N co-doped C-dots, inset: the photograph of C-dots solution under UV (365 nm) irradiation. (B) FL emission spectra of S, N co-doped C-dots at different excitation wavelengths that change from 300 nm to 440 nm. (For interpretation of the references to color in this figure legend, the reader is referred to the web version of this article.)

respectively (Fig. S1B) [36, 37]. The N_{1s} peaks at 399.7 and 400.6 eV represent pyridinic and pyrrolic N atoms, respectively (Fig. S1C) [38]. Two peaks at 531.5 and 532.7 eV in the O_{1s} spectra can be attributed to C=O and C-OH groups, respectively (Fig. S1D) [39]. These results further indicate that sulfur and nitrogen are successfully doped into the C-dots.

To investigate optical properties of S, N co-doped C-dots, the UV−vis absorption spectra and FL spectra of the carbon dots were recorded. As shown in Fig. 2A, the as-synthesized C-dots have a strong absorption peak at 335 nm, which is typically attributable to the n-π^* transition of the C=O bond [40]. The S, N co-doped C-dots solution exhibits bright blue FL under UV (365 nm) excitation (inset in Fig. 2A). FL spectra of S, N co-doped C-dots are given in Fig. 2A. The S, N co-doped C-dots show a maximum emission at 448 nm with excitation wavelength at 360 nm. To further study the FL properties of the S, N co-doped C-dots, the FL spectra of S, N co-doped C-dots were measured under different excitation wavelengths. As shown in Fig. 2B, the emission peaks do not shift under various excitation wavelengths that rang from 300 nm to 440 nm. Like other reported C-dots, the excitation-independent fluorescence characteristic may be related to less surface defects of the doped C-dots [41]. As shown in Fig. S2, the FLQY of the prepared S, N co-doped C-dots is calculated to be about 73.1% by using quinine sulfate as a standard (quantum yield of 54%). The as-prepared C-dots exhibit very high FLQY, possibly resulting from the synergy effect of the doped nitrogen and sulfur atoms [42].

Otherwise, to investigate the stability, FL intensity of the C-dots solution under extreme pH, high NaCl concentration or long time illumination was measured. The experimental results suggest that the C-dots solution owns well properties of acid resistance, alkaline resistance, salt stability, photo-stability and resistance to photo-bleaching (Fig. S3).

3.2. *FL quenching mechanism of S, N co-doped C-dots in the presence of H_2O_2 and Fe^{2+}*

FT-IR spectra and XPS spectra show that there are number of –OH, $–NH_2$ and C–S on the surface of the C-dots which play very significant roles in the stability of C-dots. The surface –OH, $–NH_2$ and C–S on C-dots are reductive groups. We speculate that the C-dots are sensitive to some strong oxidizing substances. We investigated the effect of H_2O_2 and Fe^{2+} to the FL of S, N co-doped C-dots. As shown in Fig. 3, the FL intensity of C-dots do not change after adding a certain quantity H_2O_2 or Fe^{2+}, which indicates that the presence of H_2O_2 or Fe^{2+} has little effect on the FL of C-dots

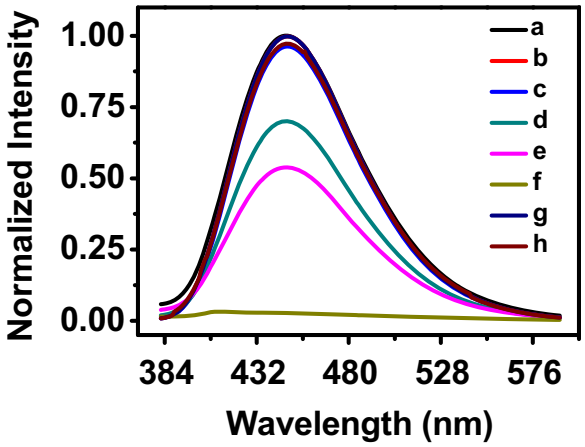

Fig. 3. FL spectra of S, N co-doped C-dots solution. The curve a represents S, N co-doped C-dots solution. The curve b represents S, N co-doped C-dots containing Fe^{2+}. The curve c represents S, N co-doped C-dots solution containing H_2O_2. The curve d represents S, N co-doped C-dots solution containing DMSO, Fe^{2+} and H_2O_2. The curve e represents the oxidized S, N co-doped C-dots solution containing $NaBH_4$. The curve f represents S, N co-doped C-dots solution containing Fe^{2+} and H_2O_2. The curve g represents S, N co-doped C-dots solution containing DMSO. The curve h represents S, N co-doped C-dots solution containing DMSO and H_2O_2. [C-dots]: 0.02 mg mL^{-1}. [Fe^{2+}]: 1 mM · [H_2O_2]: 1 mM. [DMSO]: 1 mM. [$NaBH_4$]: 1 mM. The excitation wavelength is 356 nm.

(curve c and curve b, respectively). As shown at curve f in Fig. 3, however, the FL intensity of the S, N co-doped C-dots is quenched clearly in the presence of H_2O_2 and Fe^{2+} (Fig. 3). It is well known that Fe^{2+} reacts with H_2O_2 to yield the highly reactive hydroxyl radical in acid. The oxidant capability of hydroxyl radical is stronger than H_2O_2. Therefore, we speculate that the reductive groups on C-dots surface are sensitive to highly reactive hydroxyl radicals produced from Fenton reaction of H_2O_2 and Fe^{2+} [43], which lead to effective FL quenching and change the surface states of the C-dots. Furthermore, to prove the involvement of hydroxyl radicals in the oxidation of the C-dots, dimethyl sulfoxide (DMSO, which acts as a trapping agent of hydroxyl radical), H_2O_2 and Fe^{2+} were added to the C-dots solution. As shown at curve d in Fig. 3, the FL of the prepared C-dots is recovered to a certain degree. However, the FL of the prepared C-dots has little change when C-dots solution and C-dots solution containing H_2O_2 respectively mix with DMSO (curve g and curve h). These results indirectly indicate that the obtained hydroxyl radical result in FL quenching of the C-dots. Many studies have been reported that the FL properties of C-dots are obviously affected by their surface states

[44,45]. Therefore, we deduce that the C-dots FL response to hydroxyl radical is resulted from the surface state changes of C-dots caused by the oxidation of reductive groups with hydroxyl radical. To prove this hypothesis, the fluorescent intensity of the C-dots oxidized by hydroxyl radical could be recovered was also studied. As shown at curve e in Fig. 3, the FL of the prepared C-dots is recovered to a certain degree when sodium borohydride ($NaBH_4$) were added into the solution of the C-dots oxidized with hydroxyl radical, indicating that the FL of the C-dots was related to the groups on the surface of C-dots.

Fourier transform infrared spectra (FT-IR), X-ray photoelectron spectroscopy (XPS) and zeta potential of S, N co-doped C-dots before and after reaction with H_2O_2 and Fe^{2+} were also performed. As shown in Fig. S4, compared to the original S, N co-doped C-dots (curve a), the intensity of the peak at 1647 cm^{-1} and 1405 cm^{-1}, which relate to the asymmetric and symmetric stretching vibration of carboxyl acid groups on the oxidized S, N co-doped C-dots surface (curve b), obviously increase. Compared with the original C-dots, the new peak at 1145 cm^{-1} might be identified as the stretching vibration absorption peak of the S=O and S–O band. The data of FT-IR spectra demonstrated that the –OH and C-S groups had being oxidized into $–COO^-$ and S-O, respectively. Furthermore, compare to the XPS results of S, N co-doped C-dots before reaction H_2O_2 and Fe^{2+} (Fig. S1A, Fig. S1B, Fig. S1C and Fig. S1D), after reaction the S_{2p} spectra at 164.0 eV disappear (Fig. 4A), while the spectra area of S_{2p} spectra at 167.6 eV increases (Tab. S2). The result further indicate that –C–S– is oxidized into $–C–SO_x$ (x=2, 3, 4). The spectra area of –C=O from C_{1s} and O_{1s} scan spectra obviously increase (Fig. 4B, D and Tab. S2), indicating the C-OH is oxidized into –C=O. The spectra area of pyridinic N and pyrrolic N decrease (Tab. S2), while a new peak at 403.0 eV (Fig. 4C) ($–NO_2$ group [46]) appears, suggesting the $–NH_2$ is oxidized into $–NO_2$. These above results demonstrate that –OH, $–NH_2$ and C–S are oxidized into $–COO^-$ $–NO_2$ and $–C–SO_x$, respectively. The decrease of zeta potential of S, N co-doped C-dots from −7.1 to −10.4 mV further suggests that the surface states of the C-dots are obviously changed after reaction with H_2O_2 and Fe^{2+} (see Fig. S5). Therefore, these results verified our hypothesis that the surface oxidation of S, N co-doped C-dots result in FL quenching.

3.3. Optimization of experimental conditions and the detection of uric acid

The FL of S, N co-doped C-dots was quenched apparently by hydroxyl radicals from Fenton reaction between H_2O_2 and Fe^{2+}. H_2O_2 is the main product of the uricase-catalyzed reaction. The sensitive detection of based on S, N co-doped C-dots made it possible to extend the present sensor system to the determination of UA. Therefore, the detection of UA can be performed combining two reactions. 1) H_2O_2 is generated from enzymatic reaction process of UA. 2) Fe^{2+} is introduced into the solution to construct Fenton reaction to quench the FL intensity of C-dots. To improve the sensitivity of the proposed biosensor for the detection of UA, two aspects about conditions of Fenton reaction and enzymatic reaction were studied as follows:

For Fenton reaction, the optimization of experimental conditions such as pH value, Fe^{2+} levels and incubation time, is necessary. The pH effect was studied by monitoring the dependence of the F/F_0 on the different pH values (Fig. 5A). These results suggest that the F/F_0 reaches the lowest value at pH 4.0. That is because H_2O_2 can most efficiently produce hydroxyl radicals [47,48]. Therefore, the buffer of pH 4.0 is used in this experiment. The dependence of FL-quenched efficiency by Fe^{2+} on the Fenton reaction was also investigated (Fig. 5B). The F/F_0 decreases to the minimum value at 0.3 mM. Hence, the optimum concentration of

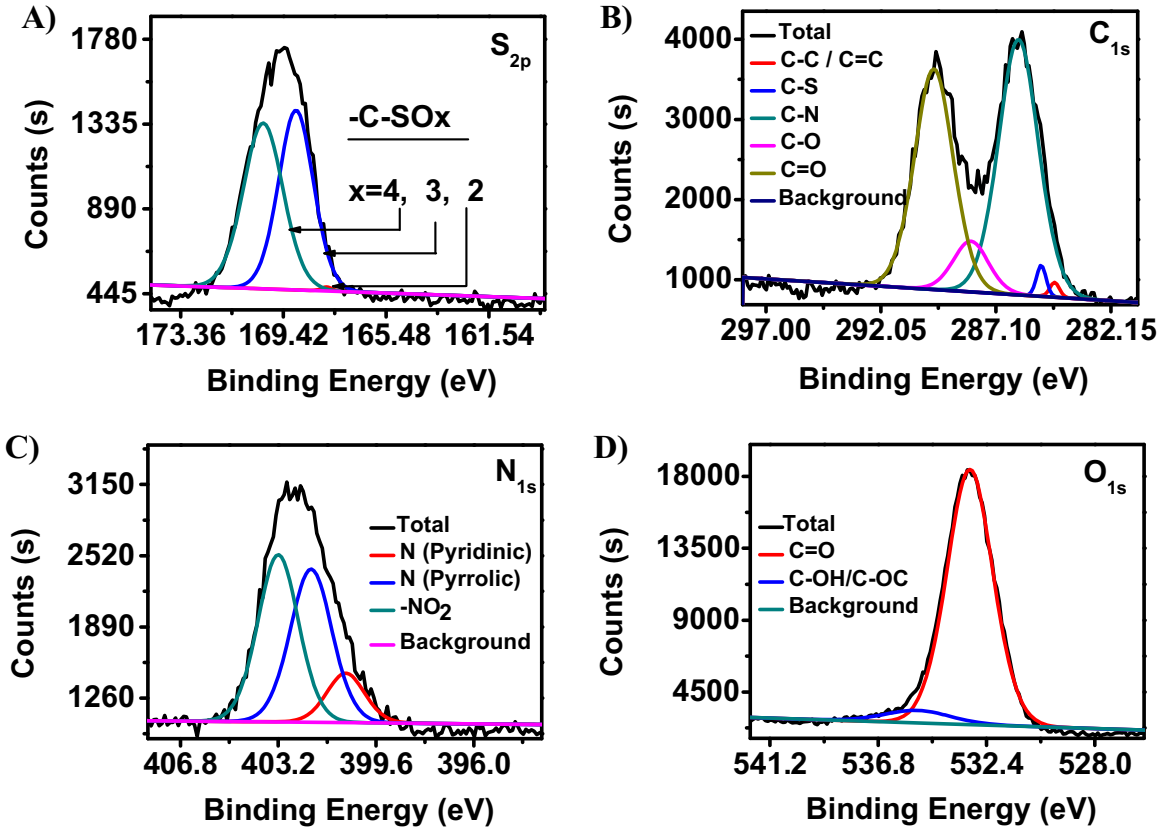

Fig. 4. High-resolution XPS of (A) S2p, (B) C1s, (C) N1s, and (D) O1s of S, N co-doped C-dots after reaction with H_2O_2 and Fe^{2+}.

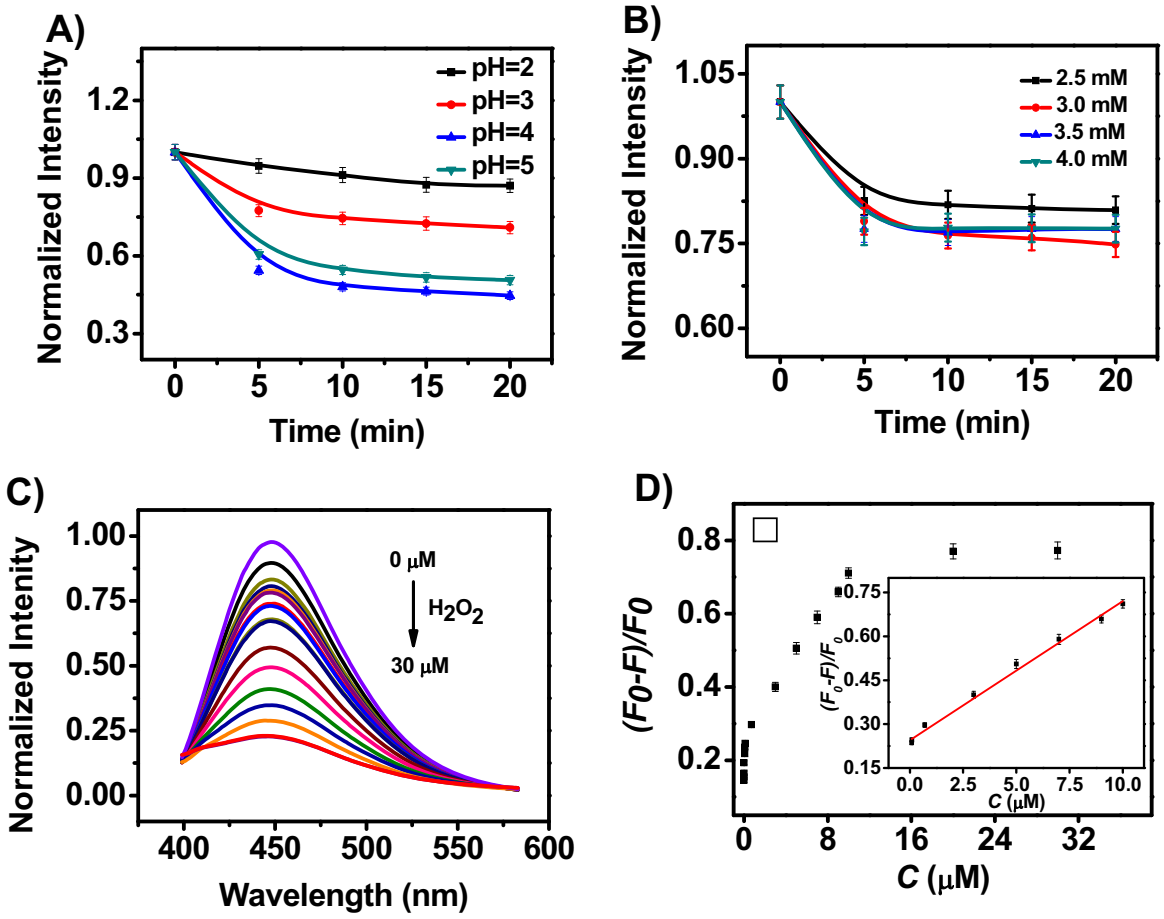

Fig. 5. The effects of (A) pH and (B) Fe^{2+} concentration on fluorescence quenching of S, N co-doped C-dots in the presence of H_2O_2 and Fe^{2+}. (C) Fluorescence emission spectra of S, N-doped C-dots in different concentrations of H_2O_2 solution in the presence of Fe^{2+} under room temperature. The concentration of S, N co-doped C-dots is 0.02 mg mL^{-1}, the concentration of Fe^{2+} is 0.3 mM, the incubation time is 15 min, pH value is 4.0 and excitation wavelength is 356 nm. (D) Quenching ratio of fluorescence for various concentration of H_2O_2. F_0 and F are the FL intensity of N-doped C-dots in the absence and presence of both H_2O_2 and Fe^{2+}, respectively. The inserted shows a linear relationship with respect to FL quenching ratio and H_2O_2 concentration.

Fe^{2+} is decided as being 0.3 mM. The F/F_0 changes slightly 15 min later (Fig. 5A and B), so 15 min is chosen as the appropriate time for the quenching process at Fenton reaction system. As shown in Fig. 5C and D, under the optimum experimental conditions, a good linear relationship for H_2O_2 concentration in the range of 0.09–10 μM is obtained by plotting $(F_0-F)/F_0$ versus the concentration of H_2O_2.

For enzymatic reaction, the effects of UA (3 μM) and uricase (1 ng mL^{-1}) to S, N co-doped C-dots were investigated. As shown in Fig. S6, the FL intensity of the S, N co-doped C-dots changes inconspicuously, which indicates that UA and uricase have little impacts to the C-dots. Otherwise, uricase and incubation time of enzymatic reaction are optimized. The influence of the concentration of uricase was investigated upon quenched FL intensity. As shown in Fig. 6A, the F/F_0 reaches minimum when the level of uricase is 1.3 U mL^{-1}. Therefore, UA level of 1.3 U mL^{-1} is used in this experiment. As shown in Fig. 6B, the FL quenching intensity reaches lowest under the reaction time of 45 min. This result suggests that the incubation time of enzymatic reaction at 45 min is used in this experiment.

Under the optimum experimental conditions, the analytical performance of detection system for quantitative detection of UA was evaluated. As shown in Fig. 6C, the FL intensity S, N co-doped C-dots at 448 nm gradually decreases with increasing concentration of UA. The FL-quenched efficiency versus the concentration of UA was shown in Fig. 6D. The calibration curve for UA has good linearity for concentrations ranging from 0.08 to 10 μM and 10–50 μM with the following equation: $(F_0-F)/F_0=0.14+0.03$ C and $(F_0-F)/F_0=0.44+0.005$ C, and their correlation coefficients are 0.991 and 0.998, respectively. The detection limit is as low as 0.07 μM (S/N=3), which is lower than of the some reported methods for melamine (Tab. S3).

3.4. Selectivity of proposed biosensor

The study of selectivity is of great importance for the biosensor. Thus, the effects of mental ions ($K^+$and Na^+) and small biological molecules (UA, AA, DA, Hcys, Cys, GSH, Lys, lactose, glucose and Leu) were investigated (Fig. 7). These results indicate that above interfering species are negligible compared with that of UA. The high selectivity could be attributed to the high affinity of uricase for UA. These results proved that the proposed biosensor could selectively detect the concentration of UA and offer credible results even the interfering species reach high concentrations.

3.5. Analysis of practical samples

To demonstrate the feasibility of the practical application of this sensing system, the proposed method was applied to detect UA levels in human serum samples. Furthermore, the concentration of UA in each sample was also analyzed using an instrument (Hitachi 7100 Automatic Biochemical Analyzer) of Hospital of Hunan Normal University to test the accuracy of this method. The UA concentrations in serum detected by the proposed assay and

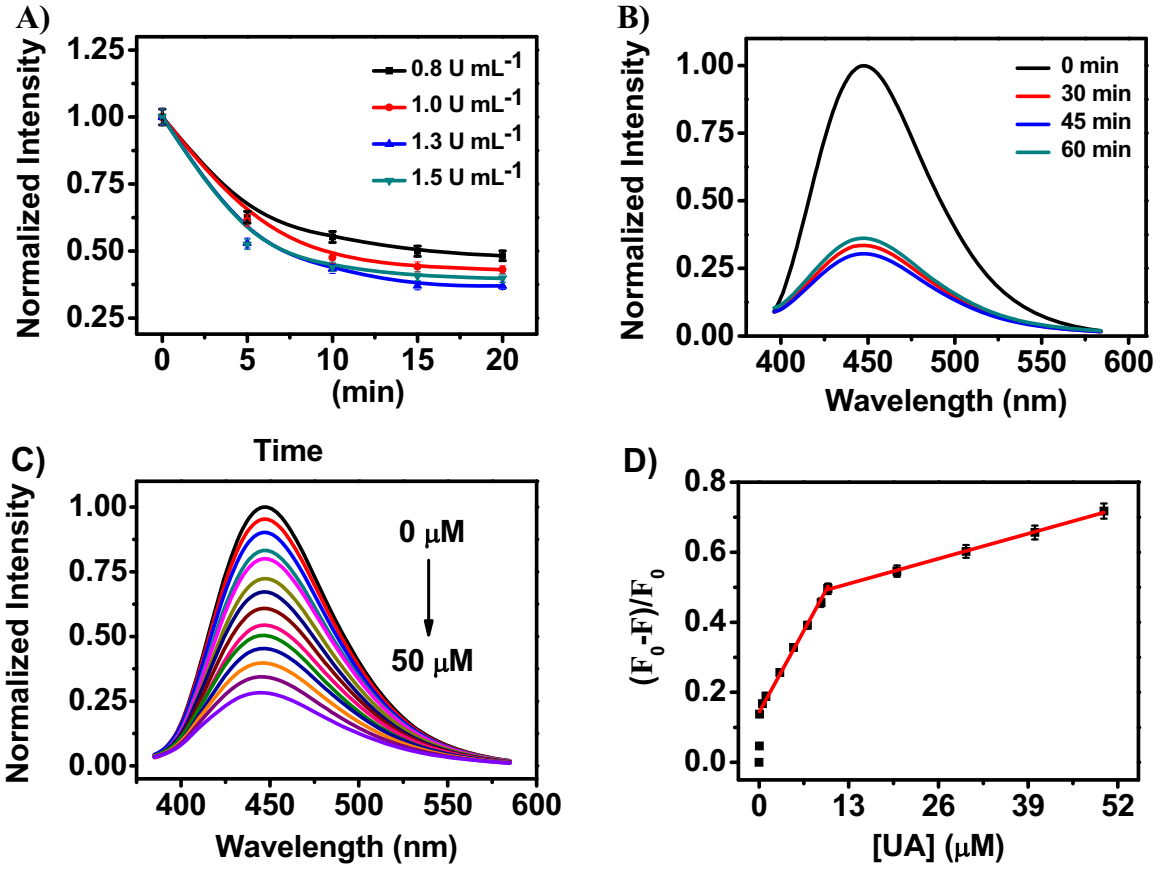

Fig. 6. (A) The effect of various concentration of uricase and (B) different incubation time of enzyme reaction for FL quenching of S, N co-doped C-dots in the presence of H_2O_2 and Fe^{2+}. (C) FL emission spectra of S, N-doped C-dots for different concentrations of UA. (D) Quenching ratio of FL for various concentration of UA. The inserted picture shows a linear relationship with respect to quenching ratio and UA level. The concentration of C-dots is 0.02 mg mL^{-1}. The excitation wavelength is 356 nm. The incubation time of Fenton reaction is 15 min. F_0 and F are the FL intensity of N-doped C-dots in the absence and presence of both H_2O_2 and Fe^{2+}, respectively.

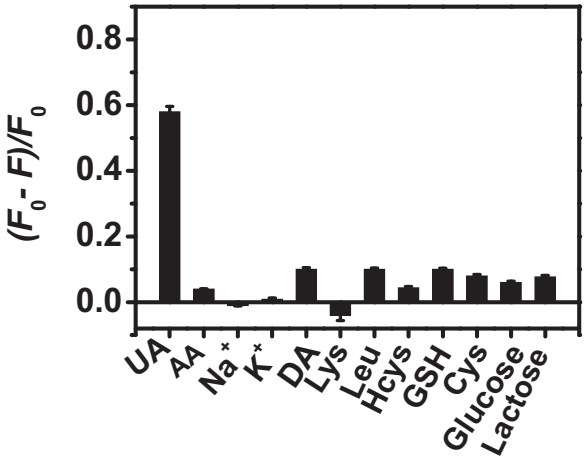

Fig. 7. Selectivity analysis for uric acid detection by quenched FL intensity of S, N co-doped C-dots. All the analytes were first incubated with uricase (1.3 U mL^{-1}) in PBS (0.1 M, pH=7.0) for 45 min at 37 °C bath. The concentration of C-dots is 0.02 mg mL^{-1}. The concentration of UA is 10 μM. The concentration of the others is 50 μM. The incubation time of Fenton reaction is 15 min.

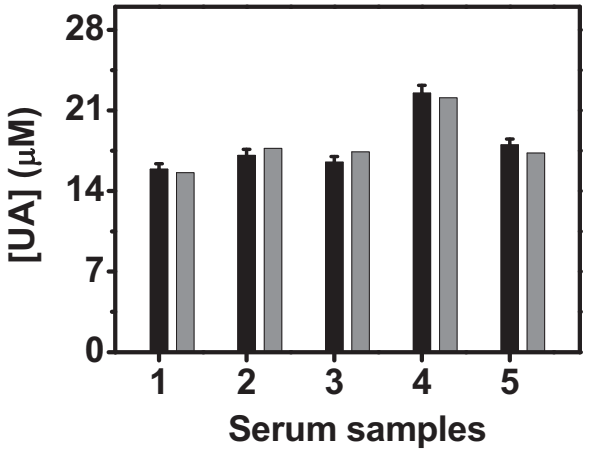

Fig. 8. Analytical results of UA in serum obtained by S, N co-doped C-dots based on FL assay and Hitachi 7100 Automatic Biochemical Analyzer. The black histograms represent results obtained by the FL method based on S, N co-doped C-dots. The gray histograms represent results obtained by the Hitachi 7100 Automatic Biochemical Analyzer. All the samples were first incubated with uricase (1.3 U mL^{-1}) in PBS (0.1 M, pH=7.0) for 45 min at 37 °C bath. The concentration of C-dots is 0.02 mg mL^{-1}. The incubation time of Fenton reaction is 15 min. The excitation wavelength is 356 nm.

Hitachi 7100 Automatic Biochemical Analyzer are shown in Fig. 8. The results obtained by the proposed method coincided well with those obtained by the instrument (Hitachi 7100 Automatic Biochemical Analyzer), indicating that the proposed assay can be successfully applied for detecting UA levels in serum samples.

4. Conclusions

In summary, high FL S, N co-doped C-dots were simply prepared using a hydrothermal method with CA and thiourea as precursors. The as-prepared C-dots have excellent FL properties

and high stability. The FL of S, N co-doped C-dots was quenched apparently by hydroxyl radicals from Fenton reaction between H_2O_2 and Fe^{2+}. UA can be oxidized by uricase to product H_2O_2. On the basis of the production of H_2O_2 coupled with FL quenching of S, N co-doped C-dots in the presence of H_2O_2 and Fe^{2+}, a simple and eco-friendly nanosensor based on S, N co-doped C-dots was developed for the detection of UA. The constructed nanosensor has some remarkable advantages of high selectivity, fast response and wide response range, which make it apply to the determination of UA in real samples. We believe that the production of high FL S, N co-doped C-dots have a significant application prospect in biological detection and biological imaging.

Acknowledgments

This work was supported by the National Natural Science Foundation of China (21275051, 21475043), Doctoral Fund of Ministry of Education of the People's Republic of China (No: 20134306110006), Hunan Provincial Science and Technology Department (No. 2014FJ6034).

Appendix A. Supplementary material

Supplementary data associated with this article can be found in the online version at http://dx.doi.org/10.1016/j.talanta.2016.04.020.

References

[1] W. Guan, X. Duan, M.A. Reed, Biosens. Bioelectron. 51 (2014) 225–231.
[2] N. Misra, V. Kumar, L. Borde, L. Varshney, Sens. Actuators B 178 (2013) 371–378.
[3] M.W. Rich, Am. J. Cardiol. 85 (2000) 1018–1021.
[4] G. Würzner, J.-C. Gerster, A. Chiolero, M. Maillard, C.-L. Fallab-Stubi, H. R. Brunner, M. Burnier, J. Hypertens. 19 (2001) 1855–1860.
[5] N. Cooper, R. Khosravan, C. Erdmann, J. Fiene, J.W. Lee, J. Chromatogr. B 837 (2006) 1–10.
[6] G. Öhman, Clin. Chim. Acta 95 (1979) 219–226.
[7] D. Huang, Y. Cheng, H. Xu, H. Zhang, L. Sheng, H. Xu, Z. Liu, H. Wu, S. Fan, J. Solid State Electrochem. 19 (2015) 435–443.
[8] M. Amjadi, J.L. Manzoori, T. Hallaj, J. Lumin. 153 (2014) 73–78.
[9] P. Xu, R. Li, Y. Tu, J. Yan, Talanta 144 (2015) 704–709.
[10] V. Kumar, N. Misra, J. Paul, B.R. Dhanawade, L. Varshney, Polymer 55 (2014) 2652–2660.
[11] T. Zhang, X. Sun, B. Liu, Spectrochim. Acta A Mol. Biomol. Spectrosc. 79 (2011) 1566–1572.
[12] Y. Xu, M. Wu, Y. Liu, X.Z. Feng, X.B. Yin, X.W. He, Y.K. Zhang, Chemistry 19 (2013) 2276–2283.
[13] H. Li, Y. Zhang, L. Wang, J. Tian, X. Sun, Chem. Commun. 47 (2011) 961–963.
[14] V.N. Mehta, S. Jha, R.K. Singhal, S.K. Kailasa, New J. Chem. 38 (2014) 6152–6160.
[15] P. Juzenas, A. Kleinauskas, P. George Luo, Y.-P. Sun, Appl. Phys. Lett. 103 (2013) 063701.
[16] J. Pan, Y. Sheng, J. Zhang, J. Wei, P. Huang, X. Zhang, B. Feng, J. Mater. Chem. A 2 (2014) 18082–18086.
[17] S. Yang, X. Feng, X. Wang, K. Müllen, Angew. Chem. Int. Ed. 50 (2011) 5339–5343.
[18] S.N. Baker, G.A. Baker, Angew. Chem. Int. Ed. Engl. 49 (2010) 6726–6744.
[19] D. Pan, J. Zhang, Z. Li, C. Wu, X. Yan, M. Wu, Chem. Commun. 46 (2010) 3681–3683.
[20] D. Yu, E. Nagelli, F. Du, L. Dai, J. Phys. Chem. Lett. 1 (2010) 2165–2173.
[21] Z. Qian, X. Shan, L. Chai, J. Ma, J. Chen, H. Feng, ACS Appl. Mater. Interfaces 6 (2014) 6797–6805.
[22] Z. Yang, M. Xu, Y. Liu, F. He, F. Gao, Y. Su, H. Wei, Y. Zhang, Nanoscale 6 (2014) 1890–1895.
[23] J. Zhou, X. Shan, J. Ma, Y. Gu, Z. Qian, J. Chen, H. Feng, RSC Adv. 4 (2014) 5465–5468.
[24] X. Shan, L. Chai, J. Ma, Z. Qian, J. Chen, H. Feng, Analyst 139 (2014) 2322–2325.
[25] F. Li, C. Liu, J. Yang, Z. Wang, W. Liu, F. Tian, RSC Adv. 4 (2014) 3201–3205.
[26] J.P. Paraknowitsch, Y. Zhang, B. Wienert, A. Thomas, Chem. Commun. 49 (2013) 1208–1210.
[27] Z. Ma, H. Ming, H. Huang, Y. Liu, Z. Kang, New J. Chem. 36 (2012) 861–864.
[28] Z.L. Wu, P. Zhang, M.X. Gao, C.F. Liu, W. Wang, F. Leng, C.Z. Huang, J. Mater. Chem. B 1 (2013) 2868–2873.
[29] J. Huang, Q. Zheng, J.-K. Kim, Z. Li, Biosens. Bioelectron. 43 (2013) 379–383.
[30] S. Mohapatra, S. Sahu, N. Sinha, S.K. Bhutia, Analyst 140 (2015) 1221–1228.
[31] S. Chandra, P. Patra, S.H. Pathan, S. Roy, S. Mitra, A. Layek, R. Bhar, P. Pramanik, A. Goswami, J. Mater. Chem. B 1 (2013) 2375–2382.
[32] S. Mohapatra, S. Sahu, N. Sinha, S.K. Bhutia, Analyst 140 (2015) 1221–1228.
[33] D. Sun, R. Ban, P.-H. Zhang, G.-H. Wu, J.-R. Zhang, J.-J. Zhu, Carbon 64 (2013) 424–434.
[34] S. Yang, L. Zhi, K. Tang, X. Feng, J. Maier, K. Müllen, Adv. Funct. Mater. 22 (2012) 3634–3640.
[35] Z. Yang, Z. Yao, G. Li, G. Fang, H. Nie, Z. Liu, X. Zhou, X.A. Chen, S. Huang, ACS Nano 6 (2012) 205–211.
[36] Q. Liang, W. Ma, Y. Shi, Z. Li, X. Yang, Carbon 60 (2013) 421–428.
[37] J.P. Paraknowitsch, Y. Zhang, B. Wienert, A. Thomas, Chem. Commun. 49 (2013) 1208–1210.
[38] K. Gong, F. Du, Z. Xia, M. Durstock, L. Dai, Science 323 (2009) 760–764.
[39] Z. Qian, J. Ma, X. Shan, H. Feng, L. Shao, J. Chen, Chemistry 20 (2014) 2254–2263.
[40] J. Niu, H. Gao, J. Lumin. 149 (2014) 159–162.
[41] J. Zhou, C. Booker, R. Li, X. Zhou, T.-K. Sham, X. Sun, Z. Ding, J. Am. Chem. Soc. 129 (2007) 744–745.
[42] Y. Dong, H. Pang, H.B. Yang, C. Guo, J. Shao, Y. Chi, C.M. Li, T. Yu, Angew. Chem. Int. Ed. 52 (2013) 7800–7804.
[43] Y. Song, S. Zhu, S. Xiang, X. Zhao, J. Zhang, H. Zhang, Y. Fu, B. Yang, Nanoscale 6 (2014) 4676–4682.
[44] J. Shen, Y. Zhu, X. Yang, C. Li, Chem. Commun. 48 (2012) 3686–3699.
[45] H. Zheng, Q. Wang, Y. Long, H. Zhang, X. Huang, R. Zhu, Chem. Commun. 47 (2011) 10650–10652.
[46] L. Tian, D. Ghosh, W. Chen, S. Pradhan, X. Chang, S. Chen, Chem. Mater. 21 (2009) 2803–2809.
[47] W.H. Koppenol, Free Radic. Biol. Med. 15 (1993) 645–651.
[48] R.G. Zepp, B.C. Faust, J. Hoigne, Environ. Sci. Technol. 26 (1992) 313–319.